No respite from permafrost-thaw impacts in absence of a global tipping point

Jan Nitzbon[a,b,1], Thomas Schneider von Deimling[a], Mehriban Aliyeva[a], Sarah E. Chadburn[c], Guido Grosse[a,d], Sebastian Laboor[a], Hanna Lee[e], Gerrit Lohmann[b,f], Norman Julius Steinert[g], Simone Maria Stuenzi[a], Martin Werner[b], Sebastian Westermann[h,i], and Moritz Langer[a,j]

[a]Permafrost Research Section, Alfred Wegener Institute Helmholtz Centre for Polar and Marine Research, Potsdam, Germany; [b]Paleoclimate Research Section, Alfred Wegener Institute Helmholtz Centre for Polar and Marine Research, Bremerhaven, Germany; [c]Mathematics and Statistics, University of Exeter, UK; [d]Institute of Geosciences, University of Potsdam, Germany; [e]Department of Biology, Norwegian University of Science and Technology, Trondheim, Norway; [f]Department of Environmental Physics, University of Bremen, Bremen, Germany; [g]NORCE Norwegian Research Centre, Bjerknes Centre for Climate Research, Bergen, Norway; [h]Department of Geosciences, University of Oslo, Norway; [i]Centre for Biogeochemistry in the Anthropocene, University of Oslo, Norway; [j]Department of Earth Sciences, Vrije Universiteit Amsterdam, The Netherlands

Arctic permafrost, the largest non-seasonal component of Earth's cryosphere, contains a significant climate-sensitive carbon pool. Its potential for loss due to climatic changes leading to a global tipping point, where thawing accelerates with disproportionate impacts, remains debated. Here, we provide an integrative perspective on this question, building on a cross-disciplinary meta-analysis of literature supported by geospatial analyses of global data products and climate model output. Contrary to the existence of a global-scale tipping point, scientific evidence suggests a quasi-linear response to global warming, both from observation-based and model-based projections. While certain processes, such as talik development, thermokarst, thermo-erosion, and vegetation interactions, can drive rapid local permafrost thaw and ground ice loss, they do not accumulate to a non-linear response beyond regional scales. We conclude that there is no safety margin for Arctic permafrost where its loss would be acceptable. Instead, with each increment of global warming, more land areas underlain by permafrost will proportionally experience thaw, causing detrimental local impacts and global feedbacks.

[1]To whom correspondence should be addressed. E-mail: jan.nitzbon@awi.de

Amplified climate warming in northern high latitudes has led to warming, thawing, and in some cases complete loss of perennially frozen ground (permafrost) (1–3) and climate models project continued and widespread permafrost loss within the current century (4–6). Of major global concern upon permafrost thaw are the liberation and release of permafrost carbon into the atmosphere in the form of greenhouse gases (GHG; mainly carbon dioxide (CO_2) and methane (CH_4)), entailing a positive feedback on climate warming of yet uncertain magnitude (7, 8). Permafrost has thus been identified as an essential climate variable by the Global Climate Observing System of the World Meteorological Organisation (9). As such it is being monitored through the Global Terrestrial Network for Permafrost (10) and as part of the Earth's heat inventory (11, 12).

In the context of investigating global warming thresholds whose crossing would imply fundamental changes to major components of the Earth system, permafrost in Arctic and Boreal regions has been proposed as a potential climate tipping element (13), and more recently "permafrost collapse" has been suggested to constitute a "global core tipping element" (14). The notion of permafrost as a global climate tipping element has manifested over the past years, not only in popular media, but also in scientific literature (e.g. 15–17). In particular, several recent and widely recognized syntheses and opinion articles on climate tipping elements have emphasized this view by featuring permafrost as a cryosphere component with an associated tipping point for its rapid loss at or above a global mean surface temperature (GMST) increase of 4–6 °C compared to pre-industrial levels (14, 18–20). This view suggests a comparatively large "safety margin" in terms of global warming levels within which permafrost loss and the associated impacts would be of less concern than other tipping elements which have their tipping points already at lower warming levels. However, (13) originally noted that "no studies to date convincingly demonstrate that it [permafrost loss] is a tipping element by our definition" (see SI of (13)), because future projections of permafrost loss did not reveal threshold behavior. Since then, the representation of permafrost processes in the land surface models (LSMs) of coupled Earth System Models (ESMs) has improved in many ways (21–23) and first process-oriented modeling studies of permafrost thaw indicate a possibly strong contribution by rapid thaw processes such as thermokarst (24–26).

According to the 6th assessment report (AR6) of the Intergovernmental Panel on Climate Change (IPCC) (27, p. 728) it is yet an open question whether specific warming thresholds at which rapid or accelerated permafrost loss at planetary scale would occur exist and whether Arctic permafrost should thus be regarded as a climate tipping element (14). Here, we assess this question systematically and provide an integrative perspective based on a meta-analysis of evidence published in peer-reviewed literature since the review article by (13) across the fields of climate, permafrost, and ecosystem research. We particularly assess whether permafrost-thaw processes and feedbacks involve dynamical threshold behavior, which would give rise to an acceleration of thaw, irreversible loss of ground ice, and liberation of GHGs across spatial scales. For this, we adopt the definition of (14) of a climate tipping point (CTP) as a "change in part of the climate system [that] becomes (i) self-perpetuating beyond (ii) a warming threshold as a result of asymmetry in the relevant feedbacks, leading to (iii) substantial and widespread Earth system impacts." By this definition, dynamical properties such as bifurcation, hysteresis, or irreversibility are neither necessary nor sufficient conditions for a climate subsystem to qualify as a tipping element, while the key characteristic is a dynamical feedback giving rise to self-perpetuation after crossing of a warming threshold.

No evidence for abrupt decline in permafrost extent and carbon content

A rapid loss of near-surface permafrost (defined as permafrost within the upper 3 m of the subsurface) at a certain level of GMST increase would constitute evidence for a global-scale climate tipping point. The most accurate assessments of present-day and future near-surface permafrost distribution rely on numerical models that simulate ground temperatures in equilibrium with the climate (28, 29). In such equilibrium models, the probability for the presence of (near-surface) permafrost at a certain location is a non-linear function of the mean annual air temperature (MAAT) and surface and subsurface properties. Using maps and observations of pan-Arctic permafrost extent, Chadburn et al. (30) constrained a plausible MAAT regime where the permafrost probability decreases from 1 to 0 (Fig. 1b), and exploited this dependency to determine the global equilibrium permafrost extent as a function of GMST increase compared to pre-industrial levels (Fig. 1a). Despite the non-linear relation which holds at a local scale, the analysis suggests a quasi-linear decrease in equilibrium permafrost extent with increasing GMST levels (about $3.5 \cdot 10^6\,\mathrm{km}^2\,{}^\circ\mathrm{C}^{-1}$). Accordingly, almost all present-day near-surface permafrost would likely be lost before GMST increased above 5–6 °C, questioning the meaningfulness of a tipping point for permafrost loss beyond such warming levels as suggested earlier (19, 20).

An essentially linear relation between permafrost extent and GMST increase was also found in the simulations of the Climate Model Intercomparison Project (CMIP) Phases 5(4, 31) and 6(6, 32). We only found one study (33) reporting that one of the CMIP5 models (HadGEM2-ES) projected an abrupt decline in high-latitude soil moisture under the Representative Concentration Pathway (RCP) scenario 8.5, shortly after 2100, and suggested that this is caused by near-surface permafrost loss. In contrast, Koven et al. (4) showed a gradual decline in permafrost area simulated by HadGEM2-ES under the same future scenario. As far as we can judge, recent global simulations by LSMs and ESMs (CMIP5 and CMIP6) do not provide any evidence for an acceleration of permafrost loss at a certain global warming level. Instead, the models confirm the approximately linear relation between near-surface permafrost extent and global warming levels found with observation-constrained equilibrium approaches (30).

A less gradual but more abrupt decline might be expected for the amount of organic carbon subject to permafrost conditions due to its heterogeneous distribution across the circum-Arctic (34). However, a very gradual decline with GMST increase is also found for the circum-Arctic permafrost carbon content when combining the approach of (30) with the organic carbon content product by (34) (Fig. 1c).

Overall, the latest observation-constrained and model-based projections do not provide evidence for the existence of thresholds in global warming levels at which permafrost extent or carbon content in the northern circumpolar Arctic would decline particularly rapid or abrupt. Instead, they suggest circum-Arctic permafrost declines quasi-linearly under warming, with projections of nearly full loss of near-surface permafrost at about 5–6 °C GMST increase compared to pre-industrial levels (Fig. 1a).

Permafrost-thaw feedbacks at local-to-regional scales

Several studies have pointed out shortcomings in the representation of the physical and biogeochemical processes in the land components of ESMs (35, 36), in particular with respect to permafrost thaw and associated feedbacks (6, 32, 37). Specifically, current ESMs still lack representations of processes that can drive permafrost thaw in a non-linear way, including talik development underneath lakes (38) and at the landscape-scale (39), thermokarst activity in ice-rich permafrost (26, 40, 41), thaw-driven erosion in hillslope areas (42), or microbial heat production in organic-rich soils (43). Such local-scale processes are not ubiquitous across the permafrost region but are typically confined to certain environmental conditions such as the climatic regime, lithology including ground ice content and distribution, topography, or biome (Fig. 2). Due to the diversity of permafrost landscapes susceptible to these thaw processes and their co-distribution with anticipated patterns of climatic changes, the existence of tipping points for permafrost loss can be hypothesized which are not captured by the equilibrium models and current-generation LSMs/ESMs described above. To test this hypothesis, we subsequently review several processes that have been reported to drive rapid permafrost thaw and assess their potential to give rise to tipping behavior across spatial scales (see Table 1 for an overview).

Talik development. A talik is a layer or volume of perennially unfrozen ground in a permafrost area (44). In the discontinuous permafrost zone, talik development can cause rapid thawing and complete loss of permafrost, while closed taliks are confined under deep water bodies in the continuous permafrost zone (45). Taliks form when the cooling in winter is not enough to refreeze all of the ground that thawed in summer, induced either by disturbances such as thermokarst or wildfires (46–48), or driven by climatic changes expressed in particularly warm summers or snow-rich winters (39) (Fig. 3a). Both field and modelling studies have described talik development to exhibit threshold behavior with timescales of reversal of several years to decades due to hydro-thermal feedbacks (46, 49–51). Increased hydrological connectivity and groundwater flow in the unfrozen soil enhance heat advection from the surroundings and are thus positive feedbacks that accelerate the thawing of permafrost or delay its re-formation after the initial disturbance ceased (52, 53). Underneath large water bodies, positive feedbacks allow for talik formation and growth even in cold continuous permafrost. This is typically the case for mature thaw lakes resulting from thermokarst processes as discussed below. Overall, talik development can entail a rapid transition from a permafrost-underlain into a permafrost-free landscape within years to decades (Fig. 3d,e), and can thus be described as a local-scale tipping point. However, the potential for coherent permafrost loss at larger spatial scales is limited. Its occurrence is tied to spatially confined disturbances or environmental conditions which do not simultaneously occur at or beyond regional scales. Talik formation driven by climatic extremes such as snow-rich winters may, however, occur more widely at up to regional scales (39).

Thermokarst and thermo-erosion. Permafrost deposits that contain excess ice (ground ice exceeding the sediment's pore volume) are prone to thermokarst and thermo-erosion processes, which broadly denote the ground subsidence and terrain change as a result of excess ice melt and associated soil volume loss (54). Thermokarst may occur within years to decades and is, therefore, a form of pulse disturbance on geological timescales also referred to as "abrupt thaw" in contrast to the slow gradual thaw through active-layer deepening (7, 41, 55). A common precursor of thermokarst and thermo-erosion is the degradation of ice wedges which are the dominant form of massive ground ice across the permafrost region (40). Thawing of ice-rich permafrost or melting of massive ground ice locally results in the formation of depressions (Figure 3b,c) which are preferentially filled with insulating snow during winter and meltwater during spring, causing further ground warming and subsidence (e.g. 56).

Lake thermokarst: In poorly-drained tundra lowlands, initially small and locally confined water bodies (40, 57) can merge into larger features and eventually form thermokarst lakes (58) (Figure 3b). These have a lower surface albedo during the snow-free season, a higher heat capacity than the surrounding terrain, and transport heat more efficiently through vertical mixing. These factors result in an increased heat uptake compared to the land surface not affected by surface water, allowing for generally deeper thaw penetration and warmer ground temperatures (45) (Fig. 3d,f). Shallow bottom-freezing lakes could constitute a "meta-stable" landscape configuration as they allow for efficient cooling of the subsurface during wintertime. However, once water body depths increase above a threshold that precludes bottom-freezing during winter (about $1-3$ m depth (59)), such configurations become unstable and sub-lake permafrost thaw continues year-round and a sub-lake talik forms. Hence, the change from a bottom-fast to a floating lake-ice regime constitutes a tipping point for the evolution of the ground thermal regime underneath thaw lakes (59, 60). At the regional scale, thermokarst lake drainage is a widespread process that is competing with lake formation and expansion and appears to increase in frequency with climate warming (61, 62). It causes an immediate change in the lake bottom temperature regime and a potentially quick (years to decades) permafrost re-formation under suitable climatic conditions (51). The re-accumulation of (excess) ground ice which melted during the thermokarst phase would, however, take much longer (centuries to millennia) such that the ground ice loss due to thermokarst must be considered as largely irreversible on human timescales. The net effects of lake formation, growth, and drainage are hard to quantify as these processes happen simultaneously in thermokarst-affected landscapes. A widespread acceleration of lake formation or expansion has not been clearly observed at this point and many remote sensing studies actually point to decreases in surface water coverage in the Arctic (62–65). Accordingly, the effect of lake thermokarst landscape dynamics on regional thaw rates of permafrost remains unclear and so far there is no evidence for a lake dynamics-driven acceleration of permafrost thaw rates at or beyond the regional scale.

Thermo-erosion: In upland or foothill settings, initial depressions due to subsidence from ice loss are mechanically eroded through meltwater runoff, resulting in a range of thermo-erosional landforms that differ from thermokarst in lowlands (Figure 3c,g). In areas with ice-wedge polygons, channelized surface runoff along the trough network promotes the melting of ice wedges through heat advection (54). Preferential snow accumulation in the subsiding troughs leads to improved insulation of the ground and thus constitutes a positive thaw-feedback (56, 66). Continued ice-wedge melting can lead to the development of high-centered polygons across the landscape (40), and locally to the development of thermal erosion gullies (67, 68). In sloped terrain, melting of excess ice just below the active layer and water saturation of the active layer soils following strong precipitation events can cause the detachment and downslope transport of the active layer material, exposing the permafrost underneath and driving rapid thaw locally (54, 69–71). Thick ice-rich deposits with large syngenetic ice wedges formed under glacial climate conditions, as well as permafrost with buried massive ice along the former margins of ice sheets, are prone to the development of retrogressive thaw slumps, which are up to kilometre-scale landforms that affect permafrost up to several tens of meters depths and develop over several years to decades (54, 72–74). In the upslope part of thermo-erosion landforms, the combination of lateral sediment transport and removal, direct exposure of ground ice to solar radiation ("thermo-denudation"), and heat transported with surface runoff entails positive feedback driving rapid permafrost thaw as well as irreversible ground ice loss and geomorphic change (75). Further downslope, sediment and debris deposition as well as ecological succession can constitute negative feedback, allowing for the stabilization of these landforms on multi-year timescales (54, 76, 77). Thermo-erosion landforms are becoming more abundant in number and affected area in many regions as documented with remote sensing studies and a further increase could be expected with the observed rise in frequency and strength of extreme events such as heat waves or high-precipitation events (42, 61, 74, 78, 79).

Summary: Thermokarst and thermo-erosion involve positive feedbacks that can drive rapid permafrost thaw at a local scale (meters to kilometers) and for a limited period of time (days to decades), but also affect deeper deposits (tens of meters depth) for longer periods through talik development. The associated ground ice loss is irreversible on timescales of centuries to millennia, and the melt of large Pleistocene syngenetic ice wedges in Yedoma or buried remnants of the Pleistocene ice sheets is fully irreversible during the current interglacial. For some thermokarst landforms, stabilizing mechanisms such as ecological succession (e.g. 80, 81) and drainage development (e.g. 82, 83) can prevent vicious cycles of self-sustained thaw until complete permafrost loss. Thermokarst and thermo-erosion can cause local "tipping" of permafrost landscapes with associated changes in the topography, hydrology, ecosystem functions, and land-atmosphere fluxes. While recent observations do not suggest a thermokarst-driven acceleration of thaw globally, this does not preclude the existence of tipping points at higher-than-present warming levels. However, at continental-to-global scales, thermokarst disturbances occur in a spatially and temporally uncorrelated manner, making an accumulation to a gradual response much more likely. Overall, we do not see ample evidence for any specific global warming threshold at which widespread permafrost loss in the sense of a climate tipping element would occur or accelerate due to thermokarst or thermo-erosion. Instead, we expect a gradual increase in abundance, frequency, and magnitude along with shifts in the regions affected by these disturbances under a warming climate.

Vegetation change. The majority of the circum-Arctic permafrost region is covered by boreal forests (about 55% areal coverage) and tundra (84) (Figure 2). The vegetation buffers underlying permafrost from atmospheric conditions through multiple mechanisms, including shading (85), lowering wind speeds, suppressing turbulent fluxes (86), precipitation interception (87, 88), modification of the snow cover and surface albedo (89–91), higher evapotranspiration (92), and the accumulation of litter and organic layers (93). The overall insulation is controlled by the vegetation type, condition, composition, and local factors such as the topography and micro-climate (94–96). Regionally, vegetation cover insulates permafrost that is not in equilibrium with the current climate, protects relic ground ice from melting and hinders subsequent thermokarst formation (97, 98). Vegetation changes are driven by multiple factors interacting with each other (99), including increasing air temperatures and longer growing seasons (100), changes in precipitation patterns, shifts in the permafrost conditions, changing disturbances such as wildfires (90, 101–103), and local factors such as hydrology or topography. Vegetation change can affect the hydrothermal permafrost conditions, which in turn feed back on vegetation dynamics (104), thereby opening the possibility for self-perpetuation and tipping behaviour under a warming climate.

Boreal forest change: Local-to-regional disturbances (fires, droughts, pests, thermokarst) lead to abrupt shifts in forest compositions and densities, with canopy loss leading to the deepening of the active layer (96) (Figure 4a). Forests show no gradual decline in tree cover towards their limits but become less resilient and more prone to shifting to open woodland or treeless states (105). This has been observed and points to widespread non-linear biome shifts to woodland or treeless states with the potential of the loss of the insulative capacities of canopies at a regional scale (106, 107). In addition, while most boreal forests are dominated by evergreen needleleaf taxa, wide areas of the boreal permafrost on the northeastern Eurasian continent are dominated by deciduous needleleaf taxa. The needle-shedding impacts the within- and below-canopy heat and water fluxes (86, 108), the litter and organic surface layers, and the fire regime (109), resulting in different hydro-thermal regimes and shallower active layers. Active-layer deepening could lead to an increase in evergreen taxa which would cause further active-layer deepening and allow further expansion of evergreen taxa due to the preference for deeper root space and lower permafrost insulation (Fig. 4a) (96, 110).

Tundra vegetation change: Shrub growth (in terms of height and abundance) is the most observed vegetation change in the Arctic and leads to increased snow-trapping, a reduction of the surface albedo, leading to an increase in energy absorption during winter and spring (93, 104), causing ground temperature increase potentially promoting further shrub growth (90) (Fig.

4b). On the other hand, thaw depths in summer are lowered due to increased canopy shading and higher evapotranspiration, suggesting a transient protection of permafrost through shrub growth. On longer timescales, the wintertime effect is expected to dominate the response of ground temperatures (98).

Summary: Overall, we do not consider vegetation change as a mechanism for rapid permafrost loss beyond regional scales, because (i) the variation in climate and landscapes would lead to local-scale tipping at different times, (ii) vegetation effects on permafrost go in both directions and potentially counterbalance each other, and (iii) while the potential feedbacks from permafrost thaw on vegetation dynamics occur rather fast (subsidence, drying, wetting, or increased growth and composition changes due to active layer deepening), self-amplification will only occur if the number of disturbances exceeds the capacity for vegetation recovery. At a local-to-regional scale, however, an increase in disturbances can lead to a rapid decline in permafrost extent, especially where permafrost is warm (mean annual ground temperatures $> -2\,^{\circ}\mathrm{C}$) and ecosystem-protected (39). While changes in vegetation cover are in principle reversible, the loss of ecosystem-protected permafrost and the melting of relic massive ground ice would be largely irreversible within the current interglacial.

Microbial heat production. Once largely undecomposed soil organic matter stored in permafrost deposits is subjected to thawed conditions, microbes can start decomposing it (7), thereby producing heat which is released into the soil. Khvorostyanov et al. (43) hypothesized that the microbial heat release could cause further permafrost thaw, potentially leading to self-perpetuating positive feedback resulting in coherent and abrupt permafrost loss particularly in the vast Yedoma region with its ice- and carbon-rich sediments covering parts of northeast Siberia and Alaska (111). Numerical models initially provided supporting evidence for this mechanism to be relevant to the thawing of Yedoma permafrost (112, 113), such that Lenton et al. (114) considered "Yedoma permafrost" as an Arctic climate tipping element. Later, Hollensen et al. (115) reported substantial microbial heat production also in incubation experiments of organic-rich permafrost cores from Greenland, supported by simulations showing similar dynamics as for talik development (Fig. 3e). We note that these cores were taken from a "kitchen midden" in Greenland containing anthropogenically enhanced organic carbon contents, which is not representative of typical permafrost deposits. Generally, a self-driven feedback would only evolve if local microbial heat release was larger than the sensible and latent heat uptake in the vicinity of the heat source. The suggested "compost bomb"-mechanism (116), therefore, requires organic carbon stocks of very high quality and large quantity, as well as relatively low ice contents. However, these preconditions are not met in vast areas of the Arctic (Fig. 2). While Yedoma deposits, despite their Pleistocene age, contain partially labile organic carbon that is microbially available following thaw (117), suggesting that these soils could provide favorable conditions to this process, their total organic carbon concentrations are fairly low and their high ground ice content must also be considered (111, 118), which would slow down the soil warming due to the large latent heat required for melting. Using the ORCHIDEE LSM (119), (120) inferred an amplifying effect on permafrost carbon release from microbial heat production but no evidence for self-perpetuating thaw. To the contrary, (121) noted that including microbial heat release in their simulations with the JSBACH LSM did not significantly affect projections of permafrost thaw rates. While we cannot exclude the possibility of self-amplified permafrost thaw and carbon degradation from microbial heat release for favorable local site conditions, we do not see convincing evidence that this mechanism could render the entire permafrost region or even a large sub-region a (global core) tipping element in the sense of (13) or (14).

Accumulation to a quasi-linear response. To assess the susceptibility to large-scale permafrost loss, we applied the approach of (30) to different sub-regions of the permafrost region that are prone to certain permafrost thaw feedbacks (solid lines in Fig. 5 a-o). Indeed, different sub-regions show increased susceptibilities to permafrost loss at certain levels of GMST increase. For example, major parts of permafrost in ice-poor boreal uplands will be out of equilibrium at a GMST increase of about $2\,^{\circ}\mathrm{C}$ above pre-industrial levels (Fig. 5 g), while major parts of permafrost in ice-rich tundra uplands are expected to remain stable up to 2–$3\,^{\circ}\mathrm{C}$ of warming (Fig. 5 h). However, the response of equilibrium permafrost to warming becomes more and more gradual if accumulated over several sub-regions (Fig. 5 c,f,i,l,m,n) and is quasi-linear for the entire permafrost region (Fig. 5 o). Even if we assumed that complete permafrost loss would locally occur at a specific MAAT threshold (dashed curve in Fig. 1 b), the sub-region and global susceptibilities would not change substantially (dashed curves in Figs. 1 a,c and 5 a-o). Thus, despite the possibility of thresholds for rapid, irreversible, and self-perpetuating permafrost thaw on local-to-regional scales, an emergence of continental-to-global scale climate tipping points from permafrost-thaw feedbacks appears very unlikely.

The local permafrost-thaw feedbacks compiled above can entail a rapid transition from permafrost-underlain to largely permafrost-free landscapes, associated with irreversible loss of ground ice, marked shifts in vegetation composition and ecosystem functions, and substantial long-term alterations to topography and hydrology. While the abundance of these processes is often climate-controlled, they are also tied to certain environmental conditions or spatially limited to certain parts of the overall land area. For most processes, there are not only positive thaw feedbacks but also mechanisms that stabilize the landscape subsequent to the initial disturbance. Overall, the marked heterogeneity and variability of environmental conditions in northern permafrost regions result in a plethora of mechanisms and feedbacks that drive and pace the transition from permafrost-underlain to permafrost-free landscapes under climate warming. While local tipping points might be crossed in different places at different times, the accumulated trajectory of permafrost change would remain gradual.

Permafrost–climate interactions at continental-to-global scales

Thawing of Arctic permafrost can significantly alter the exchange of heat, water, and carbon between the atmosphere and land at high latitudes, affecting regional and global climate patterns (122) that potentially feed back on permafrost thaw rates.

Similarly, changes in other climate subsystems could potentially accelerate permafrost thaw rates, for example through so-called "tipping cascades" (123), where the crossing of CTPs in one subsystem would cause another to tip as well. We here particularly discuss the permafrost carbon feedback and sea-ice–permafrost interactions as potential candidates for permafrost–climate interactions which might give rise to a continental-to-global scale permafrost tipping point.

Permafrost carbon feedback. As one of several carbon cycle–climate feedbacks (124), the permafrost carbon feedback (PCF) increases global temperatures through the emission of greenhouse gases following the decomposition of freshly thawed permafrost organic carbon (7, 8, 120). Over millennia, the high-latitude permafrost region acted as a carbon sink, where plant litter were deposited into organic-rich soils and preserved from decomposition under permafrost conditions (55, 125, 126). Field studies indicate an acceleration of permafrost region carbon emission under the current climatic conditions (127, 128) with net carbon loss being the largest during the non-growing season due to increased soil respiration (129–131). However, currently, there is low confidence in the direction of recent biogeochemical changes over the pan-Arctic region (132–135) and no evidence of a non-linear response to temperature change. Models predictions range from an increase in soil carbon in the permafrost region under future climate warming to a dramatic loss of soil carbon under the same warming scenarios (5). For most models, the permafrost carbon loss in response to global warming unfolds over decades to a few centuries and is linear (5, 8). Acknowledging major shortcomings of global models to represent permafrost processes, the best estimate based on CMIP6 model projections for 21st-century carbon release due to gradual permafrost thaw in response to an increase in GMST amounts to 18 (3–41) $\mathrm{GtC\,^\circ C^{-1}}$ (27) due to CO_2 emissions, and another 2.8 (0.7–7.3) $\mathrm{GtC\,^\circ C^{-1}}$ due to CH_4 emissions (Figure 6, gradual thaw). Thermokarst-related carbon emissions on the regional-to-local scale are assumed to contribute another 40% to the simulated carbon release from gradual thaw (25) (Figure 6, with rapid thaw). The marked divergence of model projections largely stems from differences in the representation of soil physics, soil biogeochemistry, soil hydrology and snow processes (4, 32, 122, 136). Generally, these differences dominate any differences in scenarios and driving climate (137). However, even under net zero or negative emissions scenarios, permafrost carbon release may continue to increase (16, 138, 139). Temporary temperature overshoots will increase permafrost emissions as permafrost regions are exposed to warming temperatures for longer than in non-overshoot scenarios (Figure 6, overshoots), and may also enhance the abundance and magnitude of rapid local-scale thaw processes and feedbacks described above.

The PCF would qualify as a tipping process, if it was not only positive, but large enough to be self-perpetuating. For this, an initial GMST increase would have to cause GHG emissions from permafrost thaw which lead to a further GMST increase that exceeds the initial warming. A back-on-the-envelope calculation using the IPCC AR6 (27) estimates for the permafrost carbon loss in response to climate warming (21 (4–48) $\mathrm{GtC\,^\circ C^{-1}}$) and the transient climate response to cumulative carbon emissions (TCRE; 0.00165 (0.0010–0.0023) $\mathrm{^\circ C\ GtC^{-1}}$), is giving a feedback factor of 0.035 (0.004–0.110) $\mathrm{^\circ C\,^\circ C^{-1}}$, implying that the PCF is by far too small to exceed a threshold for self-perpetuation at least by the end of this century. This would still hold, if additional emissions from thermokarst or temperature overshoots were factored in (Fig. 6). Consequently, the positive effect of GHG emissions from thawing permafrost on the global climate would not cause sufficient additional thaw and corresponding further emissions to drive a self-sustained feedback cycle that would lead to rapid permafrost loss at a global scale. Overall, we assess GHG emissions from thawing permafrost to occur as threshold-free feedback of yet poorly constrained magnitude that unfolds over multiple decades to centuries rather than a rapid release over a few years.

Permafrost–sea ice interactions. It has been hypothesized that a decline in Arctic sea ice extent could cause an increase in ground temperatures and negatively affect permafrost stability in the terrestrial Arctic (140). An extended open-water period due to summer sea ice retreat would lead to an increase in heat and moisture content in the polar atmosphere. The additional heat could be transported inland and cause ground temperatures to rise and also lead to increased snow depths during late summer and early fall, resulting in enhanced insulation of the ground from cold air temperatures during winter (141). The same mechanism has also been suggested to cause thinning of lake ice in the terrestrial Arctic (142), which in turn could shift lake-ice regimes and initiate sub-lake talik formation (59). Besides the evidence from model simulations of the past (143) and present (140), evidence for a link between Arctic sea ice cover and permafrost abundance has also been found in paleo records (144). In the opposite direction, it has been suggested that increased river-to-ocean heat transport from Arctic catchments could enhance sea ice loss (145). This, in turn, would enhance ocean-to-atmosphere heat and moisture transport, further amplifying the Arctic water cycle and potentially driving permafrost thaw inland which contributes to river runoff (146). However, in light of the sparse evidence it remains speculative whether such sea-ice–permafrost interactions constitute a strong enough positive feedback to result in a tipping cascade.

Discussion

Permafrost loss or "collapse" has repeatedly been brought up as a potential climate tipping element(13, 19, 20), and was included in a recent assessment of CTPs by McKay et al. (14). Here, we have assessed comprehensively, which processes are driving permafrost thaw across spatial scales, and whether CTPs could emerge from permafrost-thaw feedbacks. At a local scale and under suitable pre-conditions, various processes including thermokarst and thermo-erosion accelerate thaw rates and cause rapid ("abrupt") permafrost loss within years to decades. Therefore, we ascribe medium confidence to the existence of local-scale tipping points for permafrost thaw (Table 1). However, we do not see ample evidence for the emergence of tipping behaviour at regional-to-continental scales from such local feedbacks. Instead, our assessment suggests that due to (i) the primary dependence on the local climate, (ii) the marked spatial heterogeneity of environmental conditions (Fig. 2), and (iii) the lack of interconnections beyond regional scales, permafrost declines gradually under climate warming with no evidence of a specific global warming threshold where thaw rates would accelerate abruptly. This is in line with the depiction of "gradual thaw" as a threshold-free feedback by (14). In this sense, global-scale permafrost loss compares well with the gradual retreat of other cryosphere components such as seasonal snow cover (147), glaciers (148), and sea ice (149, 150), although we emphasize that the loss of ground ice and organic carbon which has accumulated during past glacial periods is essentially irreversible on human time scales. The arguments brought forward by (14) for "permafrost collapse" to constitute a "global core tipping element" are not convincing in our view. According to our assessment, the "compost bomb" effect through microbial heat release requires highly favorable preconditions in terms of organic carbon quantity and quality which are not met in typical permafrost deposits. Furthermore, the large-scale abrupt drying onset upon permafrost degradation projected by (151) is not supported by any field evidence and the model results have instead been convincingly ascribed to a model artefact (44). Overall, we assess with a medium confidence level, that there is no CTP for permafrost loss at continental-to-global scale.

Even in absence of a global tipping point, it is precisely the gradual and therefore imminent unfolding of permafrost-thaw impacts that is raising urgent challenges for both science and society. For science, observations of already ongoing and rapid permafrost thaw across the Arctic (152, 153, e.g.) emphasize the demand for the employment of large-scale monitoring capacities and the improvement of modelling capabilities. In-situ and remote sensing observations must enable the quantification of permafrost thaw across the Arctic, and can aid model development through improving process-understanding and providing of validation data. Current-generation LSMs and ESMs widely lack adequate structures and processes which would allow them to represent the permafrost-thaw feedbacks discussed above (Table 1). Dedicated permafrost models and LSMs/ESMs with enhanced representations of physical and biogeochemical permafrost processes are urgently needed in order to realistically quantify recent and future permafrost thaw rates and related climate feedbacks. Model development priorities include representations of (i) subgrid-scale heterogeneities, (ii) subgrid-scale lateral fluxes, (iii) dynamic landscape disturbances such as thermokarst and wildfires, and (iv) excess ground ice dynamics.

For society at large, the significance of the question regarding the existence of a global tipping point for permafrost loss diminishes when it comes to mitigating and adapting to the immediate implications of ongoing permafrost thaw. Earlier proposed thresholds for permafrost tipping beyond 5 °C of GMST increase (19, 20) or somewhat below (14) entail the risk of being misinterpreted to imply a safety margin up to which permafrost-thaw impacts would not unfold. However, GHG emissions (8) as well as local impacts on Arctic communities (e.g. 154), infrastructure (155, 156), and ecosystems (157) are substantial already at present and they can be expected to grow proportionally with every additional amount of warming. In order to limit permafrost-thaw impacts, pathways to net-zero anthropogenic GHG emissions have to be pursued ambitiously, which is the only viable way to preserve permafrost and its frozen carbon stock on a global scale.

DATA AVAILABILITY. This work does not contain original data.

CODE AVAILABILITY. The computer code and input data used for the geospatial analyses (Figures 1 and 5) is deposited at Zenodo https://doi.org/10.5281/zenodo.8366476 (158).

ACKNOWLEDGMENTS. ML, TS, SS, and JN acknowledge funding through the BMBF project PermaRisk. JN acknowledges funding through the AWI INSPIRES program. GG was supported by the Arctic Passion project and the ESA CCI Permafrost initiative. We gratefully acknowledge the creation of illustrations by Yves Nowak (AWI Communication and Media).

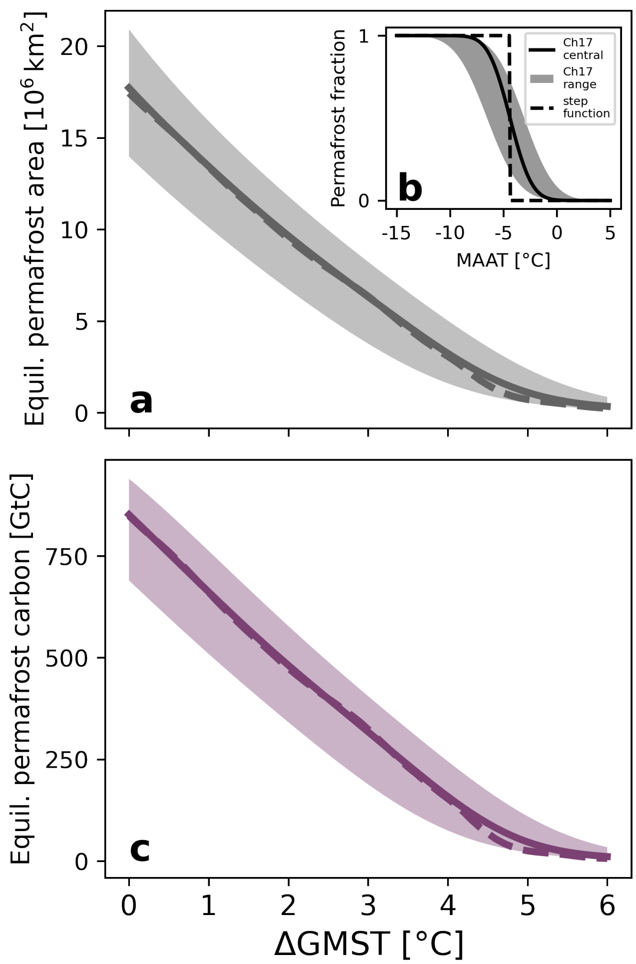

Fig. 1. a: Observation-constrained projections of equilibrium permafrost area in response to an increase in global mean surface temperature (GMST), reproduced following the same approach as Chadburn et al. (30) using ERA5-Land 2m air temperature data (1986-2005) as the climatological baseline. The approach combines a functional relationship between the local permafrost fraction and mean annual air temperature (MAAT; b) with a latitude-dependent function that scales GMST increase under consideration of Arctic amplification. The projected equilibrium permafrost area (bold line) decreases quasi-linearly with warming, without any indication of a threshold (tipping point) for rapid permafrost loss. c: According to this method and despite the globally heterogeneous distribution of soil organic carbon within the permafrost region (34), also equilibrium permafrost carbon contents would decline quasi-linearly with increasing GMST. Note, that the decline in permafrost carbon does not directly translate into carbon released into the atmosphere. The quasi-linear relations still hold, if the functional relationship between permafrost fraction and MAAT is replaced with a step function (dashed lines in a-c). Shaded areas in a and c correspond to the plausible range of the relation between permafrost fraction and MAAT by (30) shown in panel b.

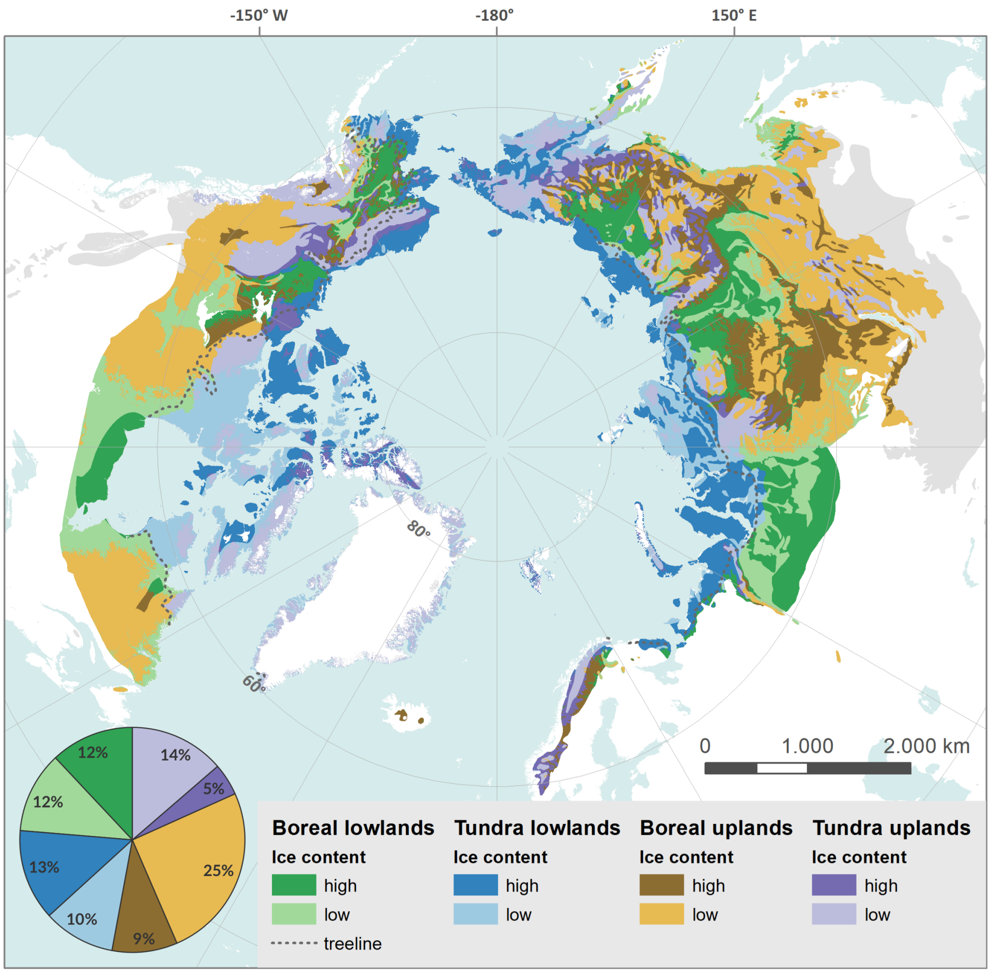

Fig. 2. Map of the northern circum-Arctic permafrost region distinguishing sub-regions according to ground ice content (high ($> 10\,\%$ excess ice, excluding massive ice), low ($\leq 10\,\%$)) according to (159), topography (lowlands (elevation ≤ 300 m above sea level), uplands (> 300 m asl)) following (160), and biome (Arctic Tundra, Boreal forest) according to (161). The pie chart in the lower left corner shows the areal fractions of the sub-regions. The processes discussed in the main text can be roughly tied to one or more of these sub-regions which provide favorable conditions (colored squares in Figures 3 and 4). The marked spatial heterogeneity of the overall circum-Arctic permafrost region eludes its depiction as a coherent planetary-scale climate subsystem.

Table 1. Compilation of processes and feedback mechanisms, which may drive rapid, irreversible, or self-perpetuating permafrost thaw at local-to-regional scales. Whether and with which confidence tipping dynamics at different spatial scales occur, is assessed on a confidence scale from −−− (no, high confidence), to ○ (neutral), to +++ (yes, high confidence).

Process	Precondition	Feedback(s) on thaw	Tipping dynamics and confidence	Timescale of reversal	Earth system impacts	Representation in LSMs/ESMs	Selected references
Talik development	Thermal disturbance (thick snowpack, deep water body, wildfire, ...)	Heat advection from groundwater flow, lake deepening through thermokarst (underneath lakes)	Local: ++; Regional: ○	Years to centuries (depending on depth)	Hydrological connectivity, Organic carbon decomposition, geomorphic change	Partly (limited depth, not underneath water bodies, not due to surface disturbance)	Fig. 3a,e; (39, 44, 49, 50)
Lake thermokarst	Ice-rich (tundra) lowlands (Fig. 2)	Lower albedo and higher heat capacity cause enhanced heat uptake	Local: ++; Regional: −	Glacial-interglacial timescale	Organic carbon mobilization and release, Hydrological cycle, geomorphic change	Experimental (3, 162)	Fig. 3b,f; (25, 26, 38, 163)
Thermo-erosion	Ice-rich uplands (Fig. 2)	Thermo-denundation and mass-wasting drive thaw; ecological succession stabilizes	Local: ++; Regional: +	Glacial-interglacial timescale	Organic carbon release and export, soil erosion and ground subsidence	Experimental (3, 162)	Fig. 3c,g; (25, 26, 42, 163)
Boreal forest change	Permafrost in boreal biome (Fig. 2), surface disturbance (e.g. wildfires)	Canopy shading and higher evaporation drive cooling and prevent thaw, Surface albedo change drives regional warming	Local: +; Regional: ○	Decades to centuries	Albedo change, Biome shift, Drought-related forest die-back	Partly (limited degree of detail, simplified plant functional types; (36))	Fig. 4a; (105, 164)
Tundra vegetation change	Permafrost in tundra biome (Fig. 2), surface disturbance (e.g. wildfires, longer growing season)	Lower albedo, higher snow pack drive ground warming, canopy shading and higher evapotranspiration drive cooling	Local: +; Regional: ○	Decades	Surface albedo change, microtopographic change, hydrologic connectivity, shrubification	Partly (limited degree of detail, simplified plant functional types; (36))	Fig. 4b; (98, 165)
Microbial heat production	Organic-rich and ice-poor soils	Heat from decomposition causes thaw of undecomposed organic matter	Local: ○; Regional: −−	Years for permafrost; Centuries for organic carbon	Organic carbon mobilization and release	Rarely (ORCHIDEE (120), JSBACH (121))	(43, 115, 120)

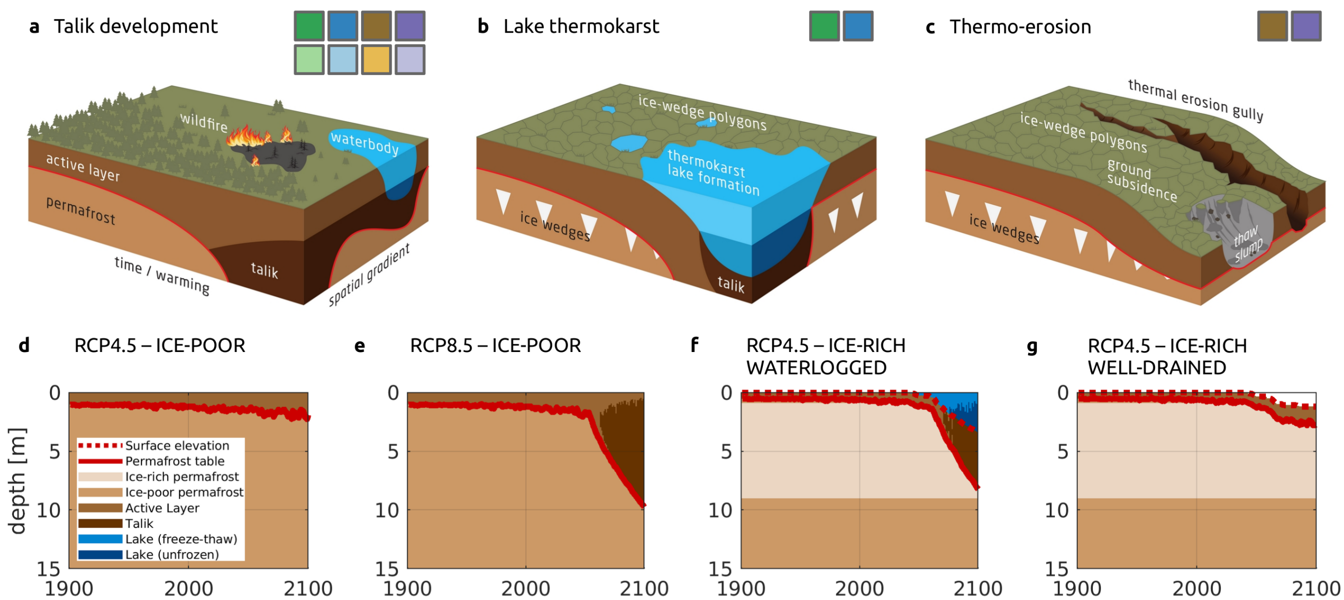

Fig. 3. a-c: Illustrations of local-scale processes driving permafrost thaw. The colored squares indicate the sub-regions in Fig. 2 where these processes predominantly occur. a: Taliks (perennially unfrozen ground surrounded by permafrost) can form due to surface disturbances (wildfires, thermokarst lakes) or climatic extremes and accelerate the transition from a permafrost-underlain into a permafrost-free landscape. b: Thermokarst lakes are abundant and actively forming in ice-rich lowlands by expanding laterally through shore erosion and into depth by forming a sub-lake talik. c: Thermo-erosion landforms are most abundant in ice-rich upland regions, where they form by the interactions between running water, melting ground ice, and sediment erosion.
d-g: Example simulations illustrating thaw dynamics under different warming scenarios and ground-ice conditions for a site in northeastern Siberia, adapted from (166). In ice-poor terrain, permafrost is projected to remain stable under moderate warming (d, RCP4.5), while rapid talik development occurs under strong warming (e, RCP8.5). In ice-rich terrain, thermokarst processes cause an acceleration of thaw, leading to the formation of a thaw lake and a sub-lake talik even under RCP4.5 and water-logged conditions (f). Under well-drained conditions and RCP4.5 (g), ground subsidence and eventual stabilization are projected for the second half of the 21st century.

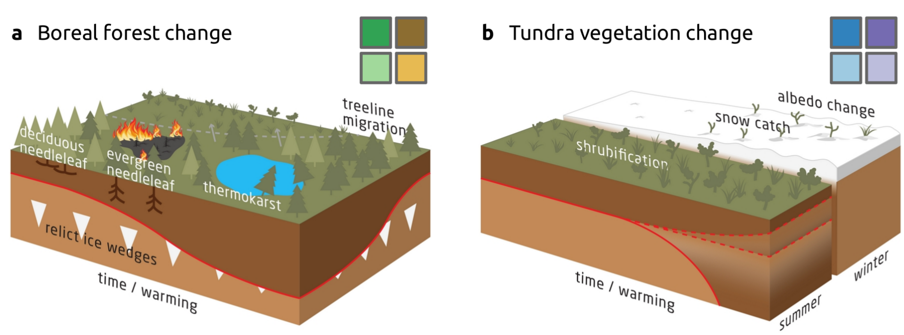

Fig. 4. Illustrations of vegetation–permafrost interactions in the Boreal (a) and Tundra (b) biomes. The colored squares indicate the sub-regions in Fig. 2 where these processes predominantly occur. a: Boreal forest change can lead to densification or loss of forest covers, or to new species compositions. Drivers include climatic changes, disturbances such as wildfires or pests, and thermokarst. Forest composition shifts are illustrated deciduous (dominant in eastern Siberia) and evergreen (dominant everywhere else) needleleaf plant functional types. b: The shrubification or greening of the tundra is driven by warming and limited by disturbances (not shown). The main implications are changes in evapotranspiration, surface albedo, and snow cover which can affect soil temperatures and thaw depths in different ways.

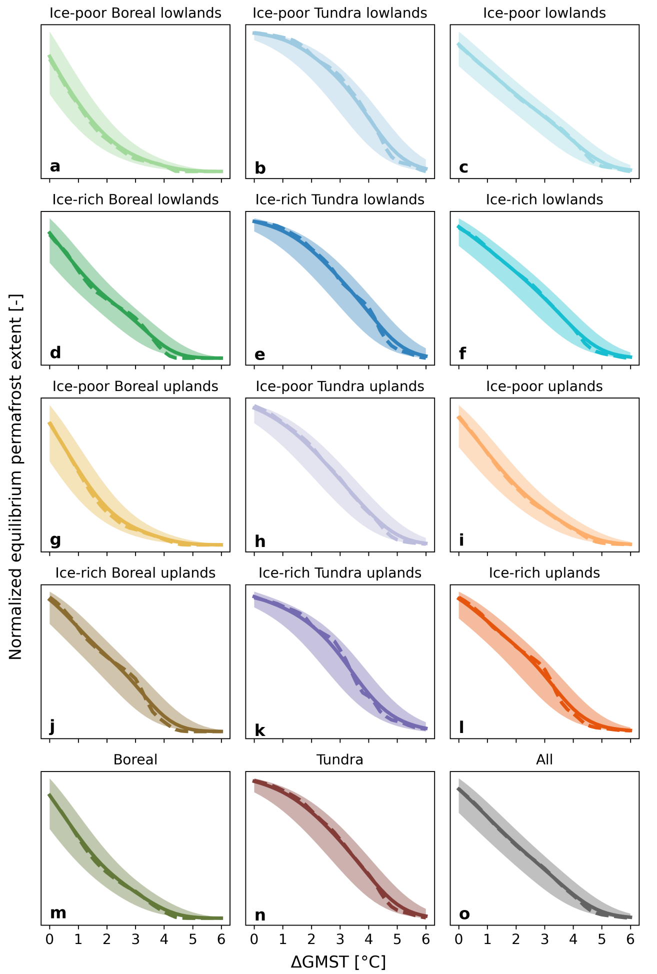

Fig. 5. Response of equilibrium permafrost extent in the sub-regions shown in Fig. 2 to an increase in global mean surface temperature (GMST), following the approach by (30). The right column and the bottom row show the combined response of the sub-regions to the left and above, respectively. Shaded areas correspond to the response within the plausible range for the relation between permafrost fraction and MAAT according to (30), dashed lines show the response if a step function is assumed (cf. Fig. 1 b). Note that a non-gradual response of equilibrium permafrost to warming does not imply a dynamical feedback mechanism driving non-linear permafrost loss.

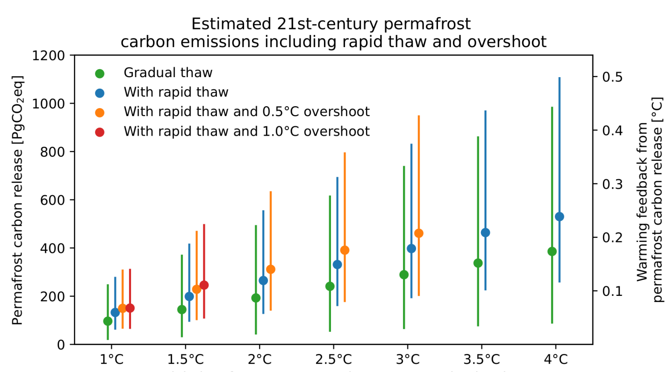

Fig. 6. Model estimates of 21st-century permafrost carbon emissions (1 GtC$=\frac{44}{12}$ PgCO$_2$eq) and the corresponding warming feedback including rapid thaw processes (i.e., thermokarst) and temperature overshoot scenarios. Gradual thaw and carbon budget estimates are from ref. (27, p. 728), rapid thaw is taken from ref. (25), and overshoot scenarios are derived from simulations in ref. (16). Error bars indicate the 5-95 $\%$ confidence interval of these estimates.

1. BK Biskaborn, et al., Permafrost is warming at a global scale. *Nat. Commun.* **10**, 264 (2019).
2. HO Pörtner, et al., eds., *IPCC Special Report on the Ocean and Cryosphere in a Changing Climate.* (Cambridge University Press, Cambridge, UK and New York, NY, USA), (2019).
3. SL Smith, HB O'Neill, K Isaksen, J Noetzli, VE Romanovsky, The changing thermal state of permafrost. *Nat. Rev. Earth & Environ.* **3**, 10–23 (2022).
4. CD Koven, WJ Riley, A Stern, Analysis of Permafrost Thermal Dynamics and Response to Climate Change in the CMIP5 Earth System Models. *J. Clim.* **26**, 1877–1900 (2013).
5. AD McGuire, et al., Dependence of the evolution of carbon dynamics in the northern permafrost region on the trajectory of climate change. *Proc. Natl. Acad. Sci.* **115**, 3882–3887 (2018).
6. EJ Burke, Y Zhang, G Krinner, Evaluating permafrost physics in the Coupled Model Intercomparison Project 6 (CMIP6) models and their sensitivity to climate change. *The Cryosphere* **14**, 3155–3174 (2020).
7. EAG Schuur, et al., Climate change and the permafrost carbon feedback. *Nature* **520**, 171–179 (2015).
8. EA Schuur, et al., Permafrost and Climate Change: Carbon Cycle Feedbacks From the Warming Arctic. *Annu. Rev. Environ. Resour.* **47**, 343–371 (2022).
9. GCOS, Permafrost Essential Climate Variable (ECV) Factsheet (2023).
10. D Streletskiy, et al., GTN-P - Strategy and Implementation Plan 2016-2020, Monograph (2017).
11. J Nitzbon, G Krinner, T Schneider von Deimling, M Werner, M Langer, First Quantification of the Permafrost Heat Sink in the Earth's Climate System. *Geophys. Res. Lett.* **50**, e2022GL102053 (2023).
12. K von Schuckmann, et al., Heat stored in the Earth system 1960–2020: where does the energy go? *Earth Syst. Sci. Data* **15**, 1675–1709 (2023).
13. TM Lenton, et al., Tipping elements in the Earth's climate system. *Proc. Natl. Acad. Sci.* **105**, 1786–1793 (2008).
14. DI Armstrong McKay, et al., Exceeding 1.5°C global warming could trigger multiple climate tipping points. *Science* **377**, eabn7950 (2022).
15. S Fabbri, MZ Hauschild, TM Lenton, M Owsianiak, Multiple Climate Tipping Points Metrics for Improved Sustainability Assessment of Products and Services. *Environ. Sci. & Technol.* **55**, 2800–2810 (2021).
16. T Gasser, et al., Path-dependent reductions in CO_2 emission budgets caused by permafrost carbon release. *Nat. Geosci.* **11**, 830–835 (2018).
17. D Yumashev, et al., Climate policy implications of nonlinear decline of Arctic land permafrost and other cryosphere elements. *Nat. Commun.* **10**, 1900 (2019).
18. TM Lenton, et al., Climate tipping points — too risky to bet against. *Nature* **575**, 592–595 (2019).
19. HJ Schellnhuber, S Rahmstorf, R Winkelmann, Why the right climate target was agreed in Paris. *Nat. Clim. Chang.* **6**, 649–653 (2016).
20. W Steffen, et al., Trajectories of the Earth System in the Anthropocene. *Proc. Natl. Acad. Sci.* **115**, 8252–8259 (2018).
21. SE Chadburn, et al., Impact of model developments on present and future simulations of permafrost in a global land-surface model. *The Cryosphere* **9**, 1505–1521 (2015).
22. A Ekici, et al., Simulating high-latitude permafrost regions by the JSBACH terrestrial ecosystem model. *Geosci. Model. Dev.* **7**, 631–647 (2014).
23. H Lee, SC Swenson, AG Slater, DM Lawrence, Effects of excess ground ice on projections of permafrost in a warming climate. *Environ. Res. Lett.* **9**, 124006 (2014).
24. T Schneider von Deimling, et al., Observation-based modelling of permafrost carbon fluxes with accounting for deep carbon deposits and thermokarst activity. *Biogeosciences* **12**, 3469–3488 (2015).
25. MR Turetsky, et al., Carbon release through abrupt permafrost thaw. *Nat. Geosci.* **13**, 138–143 (2020).
26. J Nitzbon, et al., Fast response of cold ice-rich permafrost in northeast Siberia to a warming climate. *Nat. Commun.* **11**, 2201 (2020).
27. J Canadell, et al., Global Carbon and other Biogeochemical Cycles and Feedbacks in *Climate Change 2021: The Physical Science Basis. Contribution of Working Group I to the Sixth Assessment Report of the Intergovernmental Panel on Climate Change.* (Cambridge University Press, Cambridge, United Kingdom and New York, NY, USA), pp. 673–816 (2021).
28. S Gruber, Derivation and analysis of a high-resolution estimate of global permafrost zonation. *The Cryosphere* **6**, 221–233 (2012).
29. J Obu, et al., Northern Hemisphere permafrost map based on TTOP modelling for 2000–2016 at 1 km2 scale. *Earth-Science Rev.* **193**, 299–316 (2019).
30. SE Chadburn, et al., An observation-based constraint on permafrost loss as a function of global warming. *Nat. Clim. Chang.* **7**, 340–344 (2017).
31. AG Slater, DM Lawrence, Diagnosing Present and Future Permafrost from Climate Models. *J. Clim.* **26**, 5608–5623 (2013).
32. CG Andresen, et al., Soil moisture and hydrology projections of the permafrost region – a model intercomparison. *The Cryosphere* **14**, 445–459 (2020).
33. S Drijfhout, et al., Catalogue of abrupt shifts in Intergovernmental Panel on Climate Change climate models. *Proc. Natl. Acad. Sci.* **112**, E5777–E5786 (2015).
34. G Hugelius, et al., Estimated stocks of circumpolar permafrost carbon with quantified uncertainty ranges and identified data gaps. *Biogeosciences* **11**, 6573–6593 (2014).
35. RA Fisher, CD Koven, Perspectives on the Future of Land Surface Models and the Challenges of Representing Complex Terrestrial Systems. *J. Adv. Model. Earth Syst.* **12**, e2018MS001453 (2020).
36. EM Blyth, et al., Advances in Land Surface Modelling. *Curr. Clim. Chang. Reports* **7**, 45–71 (2021).
37. SE Chadburn, et al., Carbon stocks and fluxes in the high latitudes: using site-level data to evaluate Earth system models. *Biogeosciences* **14**, 5143–5169 (2017).
38. K Walter Anthony, et al., 21st-century modeled permafrost carbon emissions accelerated by abrupt thaw beneath lakes. *Nat. Commun.* **9**, 3262 (2018).
39. LM Farquharson, VE Romanovsky, A Kholodov, D Nicolsky, Sub-aerial talik formation observed across the discontinuous permafrost zone of Alaska. *Nat. Geosci.* **15**, 475–481 (2022).
40. AK Liljedahl, et al., Pan-Arctic ice-wedge degradation in warming permafrost and its influence on tundra hydrology. *Nat. Geosci.* **9**, 312–318 (2016).
41. MR Turetsky, et al., Permafrost collapse is accelerating carbon release. *Nature* **569**, 32–34 (2019).
42. AG Lewkowicz, RG Way, Extremes of summer climate trigger thousands of thermokarst landslides in a High Arctic environment. *Nat. Commun.* **10**, 1329 (2019).
43. DV Khvorostyanov, P Ciais, G Krinner, SA Zimov, Vulnerability of east Siberia's frozen carbon stores to future warming. *Geophys. Res. Lett.* **35** (2008).
44. HB O'Neill, P Roy-Leveillee, L Lebedeva, F Ling, Recent advances (2010–2019) in the study of taliks. *Permafr. Periglac. Process.* **31**, 346–357 (2020).
45. G Grosse, B Jones, C Arp, 8.21 Thermokarst Lakes, Drainage, and Drained Basins in *Treatise on Geomorphology*, ed. JF Shroder. (Academic Press, San Diego), pp. 325–353 (2013).
46. K Yoshikawa, WR Bolton, VE Romanovsky, M Fukuda, LD Hinzman, Impacts of wildfire on the permafrost in the boreal forests of Interior Alaska. *J. Geophys. Res. Atmospheres* **107**, 8148 (2002).
47. CM Gibson, et al., Wildfire as a major driver of recent permafrost thaw in boreal peatlands. *Nat. Commun.* **9**, 3041 (2018).
48. DM Rey, et al., Wildfire-Initiated Talik Development Exceeds Current Thaw Projections: Observations and Models From Alaska's Continuous Permafrost Zone. *Geophys. Res. Lett.* **47**, e2020GL087565 (2020).
49. R Connon, E Devoie, M Hayashi, T Veness, W Quinton, The Influence of Shallow Taliks on Permafrost Thaw and Active Layer Dynamics in Subarctic Canada. *J. Geophys. Res. Earth Surf.* **123**, 281–297 (2018).
50. EG Devoie, JR Craig, RF Connon, WL Quinton, Taliks: A Tipping Point in Discontinuous Permafrost Degradation in Peatlands. *Water Resour. Res.* **55**, 9838–9857 (2019).
51. RC Rangel, et al., Geophysical Observations of Taliks Below Drained Lake Basins on the Arctic Coastal Plain of Alaska. *J. Geophys. Res. Solid Earth* **126**, e2020JB020889 (2021).
52. JC Rowland, BJ Travis, CJ Wilson, The role of advective heat transport in talik development beneath lakes and ponds in discontinuous permafrost. *Geophys. Res. Lett.* **38**, L17504 (2011).
53. Y Sjöberg, et al., Thermal effects of groundwater flow through subarctic fens: A case study based on field observations and numerical modeling. *Water Resour. Res.* **52**, 1591–1606 (2016).
54. SV Kokelj, MT Jorgenson, Advances in Thermokarst Research. *Permafr. Periglac. Process.* **24**, 108–119 (2013).
55. G Grosse, et al., Vulnerability of high-latitude soil organic carbon in North America to disturbance. *J. Geophys. Res. Biogeosciences* **116** (2011).
56. J Nitzbon, et al., Pathways of ice-wedge degradation in polygonal tundra under different hydrological conditions. *The Cryosphere* **13**, 1089–1123 (2019).
57. MT Jorgenson, et al., Rapid transformation of tundra ecosystems from ice-wedge degradation. *Glob. Planet. Chang.* **216**, 103921 (2022).
58. MT Jorgenson, Y Shur, Evolution of lakes and basins in northern Alaska and discussion of the thaw lake cycle. *J. Geophys. Res. Earth Surf.* **112** (2007).
59. CD Arp, et al., Threshold sensitivity of shallow Arctic lakes and sublake permafrost to changing winter climate. *Geophys. Res. Lett.* **43**, 6358–6365 (2016).
60. M Langer, et al., Rapid degradation of permafrost underneath waterbodies in tundra landscapes—Toward a representation of thermokarst in land surface models. *J. Geophys. Res. Earth Surf.* **121**, 2446–2470 (2016).
61. I Nitze, SW Cooley, CR Duguay, BM Jones, G Grosse, The catastrophic thermokarst lake drainage events of 2018 in northwestern Alaska: fast-forward into the future. *The Cryosphere* **14**, 4279–4297 (2020).
62. MJ Lara, Y Chen, BM Jones, Recent warming reverses forty-year decline in catastrophic lake drainage and hastens gradual lake drainage across northern Alaska. *Environ. Res. Lett.* **16**, 124019 (2021).
63. I Nitze, et al., Landsat-Based Trend Analysis of Lake Dynamics across Northern Permafrost Regions. *Remote. Sens.* **9**, 640 (2017).
64. BM Jones, et al., Identifying historical and future potential lake drainage events on the western Arctic coastal plain of Alaska. *Permafr. Periglac. Process.* **31**, 110–127 (2020).
65. EE Webb, et al., Permafrost thaw drives surface water decline across lake-rich regions of the Arctic. *Nat. Clim. Chang.* **12**, 841–846 (2022).
66. CR Burn, AG Lewkowicz, MA Wilson, Long-term field measurements of climate-induced thaw subsidence above ice wedges on hillslopes, western Arctic Canada. *Permafr. Periglac. Process.* **32**, 261–276 (2021).
67. E Godin, D Fortier, S Coulombe, Effects of thermo-erosion gullying on hydrologic flow networks, discharge and soil loss. *Environ. Res. Lett.* **9**, 105010 (2014).
68. A Morgenstern, et al., Thermo-erosional valleys in Siberian ice-rich permafrost. *Permafr. Periglac. Process.* **n/a** (2020).
69. AG Lewkowicz, C Harris, Morphology and geotechnique of active-layer detachment failures in discontinuous and continuous permafrost, northern Canada. *Geomorphology* **69**, 275–297 (2005).
70. C Harris, AG Lewkowicz, Form and internal structure of active-layer detachment slides, Fosheim Peninsula, Ellesmere Island, Northwest Territories, Canada. *Can. J. Earth Sci.* **30**, 1708–1714 (1993).
71. HT Mithan, TC Hales, PJ Cleall, Topographic and Ground-Ice Controls on Shallow Landsliding in Thawing Arctic Permafrost. *Geophys. Res. Lett.* **48**, e2020GL092264 (2021).
72. H Lantuit, WH Pollard, Temporal stereophotogrammetric analysis of retrogressive thaw slumps on Herschel Island, Yukon Territory. *Nat. Hazards Earth Syst. Sci.* **5**, 413–423 (2005).
73. SV Kokelj, TC Lantz, J Tunnicliffe, R Segal, D Lacelle, Climate-driven thaw of permafrost preserved glacial landscapes, northwestern Canada. *Geology* **45**, 371–374 (2017).
74. A Runge, I Nitze, G Grosse, Remote sensing annual dynamics of rapid permafrost thaw disturbances with LandTrendr. *Remote. Sens. Environ.* **268**, 112752 (2022).
75. F Günther, et al., Observing Muostakh disappear: permafrost thaw subsidence and erosion of a ground-ice-rich island in response to arctic summer warming and sea ice reduction. *The Cryosphere*

9, 151–178 (2015).
76. M Kanevskiy, et al., Degradation and stabilization of ice wedges: Implications for assessing risk of thermokarst in northern Alaska. *Geomorphology* **297**, 20–42 (2017).
77. S Zwieback, J Boike, P Marsh, A Berg, Debris cover on thaw slumps and its insulative role in a warming climate. *Earth Surf. Process. Landforms* **45**, 2631–2646 (2020).
78. TC Lantz, SV Kokelj, Increasing rates of retrogressive thaw slump activity in the Mackenzie Delta region, N.W.T., Canada. *Geophys. Res. Lett.* **35** (2008).
79. P Bernhard, S Zwieback, N Bergner, I Hajnsek, Assessing volumetric change distributions and scaling relations of retrogressive thaw slumps across the Arctic. *The Cryosphere* **16**, 1–15 (2022).
80. MT Jorgenson, et al., Role of ground ice dynamics and ecological feedbacks in recent ice wedge degradation and stabilization. *J. Geophys. Res. Earth Surf.* **120**, 2280–2297 (2015).
81. Y Chen, A Liu, X Cheng, Vegetation grows more luxuriantly in Arctic permafrost drained lake basins. *Glob. Chang. Biol.* **27**, 5865–5876 (2021).
82. J Nitzbon, et al., Effects of multi-scale heterogeneity on the simulated evolution of ice-rich permafrost lowlands under a warming climate. *The Cryosphere* **15**, 1399–1422 (2021).
83. SL Painter, ET Coon, AJ Khattak, JD Jastrow, Drying of tundra landscapes will limit subsidence-induced acceleration of permafrost thaw. *Proc. Natl. Acad. Sci.* **120**, e2212171120 (2023).
84. M Helbig, C Pappas, O Sonnentag, Permafrost thaw and wildfire: Equally important drivers of boreal tree cover changes in the Taiga Plains, Canada. *Geophys. Res. Lett.* **43**, 1598–1606 (2016).
85. JP Fisher, et al., The influence of vegetation and soil characteristics on active-layer thickness of permafrost soils in boreal forest. *Glob. Chang. Biol.* **22**, 3127–3140 (2016).
86. SM Stuenzi, et al., Sensitivity of ecosystem-protected permafrost under changing boreal forest structures. *Environ. Res. Lett.* **16**, 084045 (2021).
87. G Thomas, PR Rowntree, The Boreal Forests and Climate. *Q. J. Royal Meteorol. Soc.* **118**, 469–497 (1992).
88. OA Carpino, AA Berg, WL Quinton, JR Adams, Climate change and permafrost thaw-induced boreal forest loss in northwestern Canada. *Environ. Res. Lett.* **13**, 084018 (2018).
89. EJ Wilcox, et al., Tundra shrub expansion may amplify permafrost thaw by advancing snowmelt timing. *Arct. Sci.* **5**, 202–217 (2019).
90. H Kropp, et al., Shallow soils are warmer under trees and tall shrubs across Arctic and Boreal ecosystems. *Environ. Res. Lett.* **16**, 015001 (2020).
91. F Domine, et al., Permafrost cooled in winter by thermal bridging through snow-covered shrub branches. *Nat. Geosci.* **15**, 554–560 (2022).
92. DH Vitt, LA Halsey, SC Zoltai, The changing landscape of Canada's western boreal forest: the current dynamics of permafrost. *Can. J. For. Res.* **30**, 283–287 (2000).
93. GB Bonan, HH Shugart, Environmental Factors and Ecological Processes in Boreal Forests. *Annu. Rev. Ecol. Syst.* **20**, 1–28 (1989).
94. D Blok, et al., Shrub expansion may reduce summer permafrost thaw in Siberian tundra. *Glob. Chang. Biol.* **16**, 1296–1305 (2010).
95. I Grünberg, EJ Wilcox, S Zwieback, P Marsh, J Boike, Linking tundra vegetation, snow, soil temperature, and permafrost. *Biogeosciences* **17**, 4261–4279 (2020).
96. SM Stuenzi, et al., Thermohydrological Impact of Forest Disturbances on Ecosystem-Protected Permafrost. *J. Geophys. Res. Biogeosciences* **127**, e2021JG006630 (2022).
97. YL Shur, MT Jorgenson, Patterns of permafrost formation and degradation in relation to climate and ecosystems. *Permafr. Periglac. Process.* **18**, 7–19 (2007).
98. MMPD Heijmans, et al., Tundra vegetation change and impacts on permafrost. *Nat. Rev. Earth & Environ.* **3**, 68–84 (2022).
99. IH Myers-Smith, et al., Complexity revealed in the greening of the Arctic. *Nat. Clim. Chang.* **10**, 106–117 (2020).
100. ZA Mekonnen, et al., Arctic tundra shrubification: a review of mechanisms and impacts on ecosystem carbon balance. *Environ. Res. Lett.* **16**, 053001 (2021).
101. S Gauthier, P Bernier, T Kuuluvainen, AZ Shvidenko, DG Schepaschenko, Boreal forest health and global change. *Science* **349**, 819–822 (2015).
102. Y Liu, et al., Evaluation of the VIIRS BRDF, Albedo and NBAR products suite and an assessment of continuity with the long term MODIS record. *Remote. Sens. Environ.* **201**, 256–274 (2017).
103. J Blunden, DS Arndt, State of the Climate in 2016. *Bull. Am. Meteorol. Soc.* **98**, Si–S280 (2017).
104. MM Loranty, SJ Goetz, PSA Beck, Tundra vegetation effects on pan-Arctic albedo. *Environ. Res. Lett.* **6**, 024014 (2011).
105. M Scheffer, M Hirota, M Holmgren, EHV Nes, FS Chapin, Thresholds for boreal biome transitions. *Proc. Natl. Acad. Sci.* **109**, 21384–21389 (2012).
106. RG Pearson, et al., Shifts in Arctic vegetation and associated feedbacks under climate change. *Nat. Clim. Chang.* **3**, 673–677 (2013).
107. LT Berner, SJ Goetz, Satellite observations document trends consistent with a boreal forest biome shift. *Glob. Chang. Biol.* **28**, 3275–3292 (2022).
108. N Zhang, T Yasunari, T Ohta, Dynamics of the larch taiga–permafrost coupled system in Siberia under climate change. *Environ. Res. Lett.* **6**, 024003 (2011).
109. BM Rogers, AJ Soja, ML Goulden, JT Randerson, Influence of tree species on continental differences in boreal fires and climate feedbacks. *Nat. Geosci.* **8**, 228–234 (2015).
110. U Herzschuh, Legacy of the Last Glacial on the present-day distribution of deciduous versus evergreen boreal forests. *Glob. Ecol. Biogeogr.* **n/a** (2019).
111. J Strauss, et al., The deep permafrost carbon pool of the Yedoma region in Siberia and Alaska. *Geophys. Res. Lett.* **40**, 6165–6170 (2013).
112. DV Khvorostyanov, G Krinner, P Ciais, M Heimann, SA Zimov, Vulnerability of permafrost carbon to global warming. Part I: model description and role of heat generated by organic matter decomposition. *Tellus B: Chem. Phys. Meteorol.* **60**, 250–264 (2008).
113. DV Khvorostyanov, et al., Vulnerability of permafrost carbon to global warming. Part II: sensitivity of permafrost carbon stock to global warming. *Tellus B: Chem. Phys. Meteorol.* **60**, 265–275 (2008).
114. TM Lenton, Arctic Climate Tipping Points. *AMBIO* **41**, 10–22 (2012).
115. J Hollesen, H Matthiesen, AB Møller, B Elberling, Permafrost thawing in organic Arctic soils accelerated by ground heat production. *Nat. Clim. Chang.* **5**, 574–578 (2015).
116. S Wieczorek, P Ashwin, CM Luke, PM Cox, Excitability in ramped systems: the compost-bomb instability. *Proc. Royal Soc. A: Math. Phys. Eng. Sci.* **467**, 1243–1269 (2011).
117. LL Jongejans, et al., Molecular biomarkers in Batagay megaslump permafrost deposits reveal clear differences in organic matter preservation between glacial and interglacial periods. *The Cryosphere* **16**, 3601–3617 (2022).
118. L Schirrmeister, et al., Fossil organic matter characteristics in permafrost deposits of the northeast Siberian Arctic. *J. Geophys. Res. Biogeosciences* **116**, G00M02 (2011).
119. G Krinner, et al., A dynamic global vegetation model for studies of the coupled atmosphere-biosphere system. *Glob. Biogeochem. Cycles* **19** (2005).
120. CD Koven, et al., Permafrost carbon-climate feedbacks accelerate global warming. *Proc. Natl. Acad. Sci.* **108**, 14769–14774 (2011).
121. P de Vrese, T Stacke, T Kleinen, V Brovkin, Diverging responses of high-latitude CO_2 and CH_4 emissions in idealized climate change scenarios. *The Cryosphere* **15**, 1097–1130 (2021).
122. P de Vrese, et al., Representation of soil hydrology in permafrost regions may explain large part of inter-model spread in simulated Arctic and subarctic climate. *The Cryosphere* **17**, 2095–2118 (2023).
123. E Kriegler, JW Hall, H Held, R Dawson, HJ Schellnhuber, Imprecise probability assessment of tipping points in the climate system. *Proc. Natl. Acad. Sci.* **106**, 5041–5046 (2009).
124. M Heimann, M Reichstein, Terrestrial ecosystem carbon dynamics and climate feedbacks. *Nature* **451**, 289–292 (2008).
125. J Loisel, et al., A database and synthesis of northern peatland soil properties and Holocene carbon and nitrogen accumulation. *The Holocene* **24**, 1028–1042 (2014).
126. A Lindgren, G Hugelius, P Kuhry, Extensive loss of past permafrost carbon but a net accumulation into present-day soils. *Nature* **560**, 219–222 (2018).
127. L Bruhwiler, FJW Parmentier, P Crill, M Leonard, PI Palmer, The Arctic Carbon Cycle and Its Response to Changing Climate. *Curr. Clim. Chang. Reports* **7**, 14–34 (2021).
128. N Rößger, T Sachs, C Wille, J Boike, L Kutzbach, Seasonal increase of methane emissions linked to warming in Siberian tundra. *Nat. Clim. Chang.* **12**, 1031–1036 (2022).
129. R Commane, et al., Carbon dioxide sources from Alaska driven by increasing early winter respiration from Arctic tundra. *Proc. Natl. Acad. Sci.* **114**, 5361–5366 (2017).
130. SM Natali, et al., Large loss of CO 2 in winter observed across the northern permafrost region. *Nat. Clim. Chang.* **9**, 852–857 (2019).
131. NC Parazoo, CD Koven, DM Lawrence, V Romanovsky, CE Miller, Detecting the permafrost carbon feedback: talik formation and increased cold-season respiration as precursors to sink-to-source transitions. *The Cryosphere* **12**, 123–144 (2018).
132. EJ Dlugokencky, EG Nisbet, R Fisher, D Lowry, Global atmospheric methane: budget, changes and dangers. *Philos. Transactions Royal Soc. A: Math. Phys. Eng. Sci.* **369**, 2058–2072 (2011).
133. HD Graven, et al., Enhanced Seasonal Exchange of CO2 by Northern Ecosystems Since 1960. *Science* **341**, 1085–1089 (2013).
134. M Meredith, et al., Polar Regions in *IPCC Special Report on the Ocean and Cryosphere in a Changing Climate.* (Cambridge University Press, Cambridge, UK and New York, NY, USA), pp. 203–320 (2019).
135. BW Abbott, et al., Biomass offsets little or none of permafrost carbon release from soils, streams, and wildfire: an expert assessment. *Environ. Res. Lett.* **11**, 034014 (2016).
136. NJ Steinert, et al., Agreement of Analytical and Simulation-Based Estimates of the Required Land Depth in Climate Models. *Geophys. Res. Lett.* **48**, e2021GL094273 (2021).
137. EJ Burke, et al., Quantifying uncertainties of permafrost carbon–climate feedbacks. *Biogeosciences* **14**, 3051–3066 (2017).
138. AH MacDougall, Estimated effect of the permafrost carbon feedback on the zero emissions commitment to climate change. *Biogeosciences* **18**, 4937–4952 (2021).
139. J Schwinger, A Asaadi, NJ Steinert, H Lee, Emit now, mitigate later? Earth system reversibility under overshoots of different magnitudes and durations. *Earth Syst. Dyn.* **13**, 1641–1665 (2022).
140. DM Lawrence, AG Slater, RA Tomas, MM Holland, C Deser, Accelerated Arctic land warming and permafrost degradation during rapid sea ice loss. *Geophys. Res. Lett.* **35** (2008).
141. A Jan, SL Painter, Permafrost thermal conditions are sensitive to shifts in snow timing. *Environ. Res. Lett.* **15**, 084026 (2020).
142. VA Alexeev, CD Arp, BM Jones, L Cai, Arctic sea ice decline contributes to thinning lake ice trend in northern Alaska. *Environ. Res. Lett.* **11**, 074022 (2016).
143. AP Ballantyne, et al., The amplification of Arctic terrestrial surface temperatures by reduced sea-ice extent during the Pliocene. *Palaeogeogr. Palaeoclimatol. Palaeoecol.* **386**, 59–67 (2013).
144. A Vaks, et al., Palaeoclimate evidence of vulnerable permafrost during times of low sea ice. *Nature* **577**, 221–225 (2020).
145. H Park, et al., Increasing riverine heat influx triggers Arctic sea ice decline and oceanic and atmospheric warming. *Sci. Adv.* **6**, eabc4699 (2020).
146. P Wang, et al., Potential role of permafrost thaw on increasing Siberian river discharge. *Environ. Res. Lett.* **16**, 034046 (2021).
147. CW Thackeray, C Derksen, CG Fletcher, A Hall, Snow and Climate: Feedbacks, Drivers, and Indices of Change. *Curr. Clim. Chang. Reports* **5**, 322–333 (2019).
148. DR Rounce, et al., Global glacier change in the 21st century: Every increase in temperature matters. *Science* **379**, 78–83 (2023).
149. S Tietsche, D Notz, JH Jungclaus, J Marotzke, Recovery mechanisms of Arctic summer sea ice. *Geophys. Res. Lett.* **38** (2011).
150. KC Armour, I Eisenman, E Blanchard-Wrigglesworth, KE McCusker, CM Bitz, The reversibility of sea ice loss in a state-of-the-art climate model. *Geophys. Res. Lett.* **38** (2011).
151. B Teufel, L Sushama, Abrupt changes across the Arctic permafrost region endanger northern development. *Nat. Clim. Chang.* **9**, 858–862 (2019).
152. I Nitze, G Grosse, BM Jones, VE Romanovsky, J Boike, Remote sensing quantifies widespread abundance of permafrost region disturbances across the Arctic and Subarctic. *Nat. Commun.* **9**, 5423 (2018).

153. LM Farquharson, et al., Climate Change Drives Widespread and Rapid Thermokarst Development in Very Cold Permafrost in the Canadian High Arctic. *Geophys. Res. Lett.* **46**, 6681–6689 (2019).
154. AM Irrgang, H Lantuit, RR Gordon, A Piskor, GK Manson, Impacts of past and future coastal changes on the Yukon coast — threats for cultural sites, infrastructure, and travel routes. *Arct. Sci.* **5**, 107–126 (2019).
155. J Hjort, et al., Degrading permafrost puts Arctic infrastructure at risk by mid-century. *Nat. Commun.* **9**, 5147 (2018).
156. M Langer, et al., Thawing permafrost poses environmental threat to thousands of sites with legacy industrial contamination. *Nat. Commun.* **14**, 1–11 (2023).
157. EA Schuur, MC Mack, Ecological Response to Permafrost Thaw and Consequences for Local and Global Ecosystem Services. *Annu. Rev. Ecol. Evol. Syst.* **49**, 279–301 (2018).
158. J Nitzbon, M Aliyeva, T Schneider von Deimling, M Langer, Computer code: Response of permafrost extent and carbon content to increasing global mean surface temperature (2023) Zenodo. DOI:10.5281/zenodo.8366476.
159. J Brown, OJ Ferrians Jr., JA Heginbottom, ES Melnikov, Circum-Arctic map of permafrost and ground-ice conditions (1997).
160. BM Jones, et al., Lake and drained lake basin systems in lowland permafrost regions. *Nat. Rev. Earth & Environ.* **3**, 85–98 (2022).
161. E Dinerstein, et al., An Ecoregion-Based Approach to Protecting Half the Terrestrial Realm. *BioScience* **67**, 534–545 (2017).
162. KS Aas, et al., Thaw processes in ice-rich permafrost landscapes represented with laterally coupled tiles in a land surface model. *The Cryosphere* **13**, 591–609 (2019).
163. D Olefeldt, et al., Circumpolar distribution and carbon storage of thermokarst landscapes. *Nat. Commun.* **7**, 13043 (2016).
164. JE Holloway, et al., Impact of wildfire on permafrost landscapes: A review of recent advances and future prospects. *Permafr. Periglac. Process.* **31**, 371–382 (2020).
165. BM Jones, et al., Recent Arctic tundra fire initiates widespread thermokarst development. *Sci. Reports* **5**, 15865 (2015).
166. S Westermann, et al., Simulating the thermal regime and thaw processes of ice-rich permafrost ground with the land-surface model CryoGrid 3. *Geosci. Model. Dev.* **9**, 523–546 (2016).